# SCHEMES FOR RECONSTRUCTING THE SEISMIC RESPONSE OF INSTRUMENTED BUILDINGS

Dionisio Bernal[1] and Arash Nasseri[2]

[1]Civil and Environmental Engineering Department, Center for Digital Signal Processing, Northeastern University, Boston, MA.
[2] Graduate Student, Northeastern University, Boston, MA,

## Abstract

Methodology for reconstructing the seismic response of buildings from measured accelerations is examined. The popular cubic spline (CS) interpolation is shown to be equivalent to fitting the measured response on a basis whose dimension is equal to the number of sensors and whose span is determined by the sensor positions. The basis fitting perspective makes clear that a necessary condition for accuracy is that the number of sensors be no less than the number of modes that contribute substantially to the estimated quantity. It is shown that low pass filtering of the measured response, using a cutoff frequency in the proximity of the frequency of mode ($m$-1), where $m$ is the number of sensors, is advisable. Reconstruction by blending the measurements with a nominal model is examined using the Kalman Filter, the RTS Smoother and a new approach designated as the Minimum Norm Response Corrector (MIRC). Results obtained using 3 nonlinear building models and an ensemble of 30 bi-directional earthquake motions suggest that, for the conditions that prevail in practice, (i.e., relatively poor nominal models and possible nonlinearity in the measured response) the MIRC estimator is the most accurate. The gains in accuracy offered by MIRC over the CS are modest for inter-story drift but are significant in story shears. Specifically, the mean of predictions normalized to the true result (based on 1560 story shear histories) proved to be 1.48 for the CS and 1.00 for MIRC.

## Introduction

The need to reconstruct the response of systems given a limited number of measurements arises in many fields. In earthquake engineering, in particular, data from instrumented buildings has been used for validating seismic design codes, improving analytical models and evaluating how a motion may have affected the integrity of a structure (Li.et al. 1997, De la Llera and Chopra 1995, Ventura et al. 2000 and 2003). The traditional scheme used in building seismic response reconstruction approximates the accelerations at unmeasured levels using interpolation; linear interpolation and cubic splines being two common choices (Lui, Mahin and Mohele 1990, De la LLera and Chopra 1995, Limongelli 2003, Naeim 1997, Naeim et.al., 2006). A key limitation of all interpolation schemes, as shall be shown, is the fact that the dimension of the fitting basis is limited by the number of sensors, $m$. If there are $q$ modes that contribute significantly to a quantity, and $q > m-1$, the results from interpolation will be poor. In this regard it's worth noting that while $q < m$ -1 is necessary, it is not a sufficient condition for reconstruction accuracy because the location of the sensors and the nature of the interpolating functions also play a role.

An advantage of model based estimation over basis fitting is the fact that the basis dimension is not determined by the number of sensors. In model based estimation the discrepancies between model predictions and measurements are used to adjust the estimated response at unmeasured coordinates. Model based estimators differ depending on what is known (or assumed) about the source of the observed discrepancies. In control, for example, uncertainties are assumed to come from unmeasured inputs (typically referred to as process noise) and the model is presumed accurate. For these conditions the optimal estimator, if the disturbances are broad band, is the much celebrated Kalman Filter (Kalman 1960). The situation in the seismic response reconstruction problem, however, is one where the majority of the discrepancies come from approximation in the model itself.

An observer designed with the seismic response problem in mind, presented by Hernandez and Bernal (2008), operates by forcing the response to follow the measurements using fictive forces that are collocated with the sensor positions. A generalization of this approach designated as the Minimum Norm Response Corrector (MIRC) was developed in this project. The MIRC algorithm uses fictive forces applied at all coordinates and selects them, form the set of all the possible solutions, as those for which a certain metric related to their magnitude is minimal. An issue that arises when one considers model-based estimation research is deciding on the level of disparity between the "truth model" used to generate the data and the nominal model in the estimator. A realistic simulation of this discrepancy is particularly important in the seismic response reconstruction scenario because model error is likely the main source of uncertainty. In this project it was decided that practicality required the use of linear models, independently of whether the true response was linear or nonlinear.

## Reconstruction via Basis Fitting

Let $y_m$ and $y_u$ be the measured and the unmeasured coordinates and let *m* and *u* represent the number of coordinates in each set, the total number of coordinates is *n*=*m*+*u*. The response can be expressed as

$$\begin{Bmatrix} y_m(t) \\ y_u(t) \end{Bmatrix} = \begin{bmatrix} \Phi_{mm} & \Phi_{mu} \\ \Phi_{um} & \Phi_{uu} \end{bmatrix} \begin{Bmatrix} Y_1(t) \\ Y_2(t) \end{Bmatrix} \tag{1}$$

from where it is a simple matter to show that

$$y_u(t) = \Phi_{um}\Phi_{mm}^{-1}.y_m(t) + \left(\Phi_{uu} - \Phi_{um}\Phi_{mm}^{-1}\Phi_{mu}\right)Y_2(t) \tag{2}$$

Since $Y_2(t)$ cannot be computed, the common assumption is to take it equal to zero and predict the response at the unmeasured coordinates using the first term in eq.1. In this approach error is restricted to the unmeasured coordinates and is equal to the second term in Eq.2. As one gathers, the error is anticipated to be of high frequency and to vary along the height of the building according to the norm of the rows of the matrix in the parenthesis. When the second part of Eq.2 is negligible the estimate from part one is sufficiently accurate and all is well. In many

cases, however, error in the accelerations in the upper floors is not negligible and results can be improved notably by low pass filtering the measurements. Adding an *f* to the subscript of the measurements to indicate that they may be filtered one has

$$y(t) \cong \Psi \cdot y_{mf}(t) \tag{3}$$

where

$$\Psi = \begin{bmatrix} I \\ \Phi_{um}\Phi_{mm}^{-1} \end{bmatrix} \tag{4}$$

If the response is essentially linear the first *m-1* mode shapes (plus the rigid body mode) provide a "good" fitting basis. A practical approach to estimate these shapes without the need to formulate a detailed model, for buildings with reasonably uniform properties along the height, is to use the mode shapes of a flexural-shear continuum (Miranda and Taghavi 2005; Alimoradi et al. 2006). These shapes are determined by a single parameter that can be estimated from the ratio of natural periods or, with some practice, from experience.

**The Cubic Spline**

Schemes that reconstruct the response using prescribed interpolating functions are particular versions of the basis fitting approach. We illustrate the matter using the cubic spline interpolator, generalization to other interpolators is apparent from the derivation. The cubic spline interpolation states that the position of points in a building segment defined by any two subsequent sensors is

$$y(z,t) = e(t) + f(t)z + g(t)z^2 + h(t)z^3 \tag{5}$$

where *z* is the distance measured upwards from the lower sensor and the quadruple {*e(t), f(t), g(t), h(t)*} are time dependent coefficients. Let *m* be the number of sensors in a given direction; the number of segments is then *m*-1 and the number of constants to be identified at each time station *4(m-1).* Imposing continuity up to the second derivative at interior points one has 3(m-2) constraints, plus the *m* measurements, yielding a total of 4*m*-2 constraints. Counting unknowns and equations one concludes that two additional constraints are needed. These constraints are typically taken as a first derivative = 0 at the base and the roof or first derivative = 0 at the base and second derivative = 0 at the roof, approximations that are reasonable for shear dominated or flexure dominated structures, respectively. Note that discontinuity in the third derivative of the cubic spline at interior nodes is reasonable given that the third derivative is related to shear forces and these suffer abrupt jumps at story levels. Needless to say, discontinuity in the 3$^{rd}$ derivative at the levels located within a segment is not realized.

Let *a*(t) be the vector of all the coefficients of the cubic spline, namely {e(t),f(t),g(t),h(t)} for segment 1 followed by {e(t),f(t),g(t),h(t)} for segment 2 etc. Eliminating explicit reference to time for notational simplicity we designate the entries in this vector as $a_1, a_2,$ etc, with $a_1$-$a_4$ corresponding to the first segment, $a_5$-$a_8$ to the second, and so on. The *m* equations that relate these coefficients to the measurements can be written as

$$A_1.a = y_m \tag{6}$$

Note that at interior points one can take the upper or the lower segment to formulate the entries in the $A_1$ matrix. Selecting the upper segment is simplest since the row entries are zero except for a single value of 1. Needless to say, for the roof measurement one has to use the lower segment so the last row of $A_1$ has 4 non-zero terms.

Continuity leads to equations of the form $f$ (a) = 0. To illustrate assume that there are 3 sensors (base roof and 1 intermediate) so there are two segments. Continuity in displacement, slope and curvature at the interior point gives

$$a_1 + a_2\ell_1 + a_3\ell_1^2 + a_4\ell_1^3 - a_5 = 0 \tag{7}$$

$$a_2 + 2a_3\ell_1 + 3a_4\ell_1^2 - a_6 = 0 \tag{8}$$

$$2a_3 + 6a_4\ell_1 - 2a_7 = 0 \tag{9}$$

where $\ell_1$ is the height of the first segment. The 3(m-2) continuity equations can be grouped and written as

$$A_2.a = 0 \tag{10}$$

The boundary conditions are two equations of the form $g$ (a) = 0, for example, in the case of zero slope at the roof and the base one has (with notation for the case of two segments)

$$a_2 = 0 \tag{11a}$$

$$a_6 + 2a_7\ell_2 + 3a_8\ell_2^3 = 0 \tag{11b}$$

The equations describing the boundary conditions are, therefore

$$A_3.a = 0 \tag{12}$$

Finally, the response at all floors is linearly related to the coefficients in the vector $a$ so one can write

$$y = A_4.a \tag{13}$$

Equations 10 and 12 can be combined into

$$\begin{bmatrix} A_2 \\ A_3 \end{bmatrix} \{a\} = \{0\} \tag{14}$$

or, with obvious notation

$$A_{2,3}.a = 0 \tag{15}$$

from where it follows that

$$a = Q.v \tag{16}$$

where

$$Q = null(A_{2,3}) \tag{17}$$

Substituting the result of Eq.16 into Eq.6 and solving for *v* one gets

$$v = [A_1 \cdot Q]^{-1}.y_m \tag{18}$$

where it can be shown that the matrix in the bracket is full rank and square. Substituting Eq.18 into Eq.16 and the result into Eq.13 yields

$$y(t) = A_4 Q \cdot [A_1.Q]^{-1} y_m(t) \tag{19}$$

which shows that the cubic spline interpolation is a particular case of the basis fitting where the matrix $A_4 Q \cdot \left[A_1 Q\right]^{-1}$ plays the role of $\Psi$ (see Eq.3). Note that the basis of the CS is dictated by the interpolating function and the position of the sensors so there is no "adaptability" in the scheme. The result in Eq.19 clarifies the CS interpolation scheme and is computationally significant since it shows that there is no need to solve a set of simultaneous equations at each time step (the traditional approach) but it suffices to compute the matrix in Eq.19 (once) and the reconstruction at any time follows from a simple matrix multiplication.

**Error Measures**

To compare the accuracy of reconstructions obtained with various methods we define the following metrics where *y* is the true and $y_p$ is the predicted response.

Peak Response Indicators
PRP = max $[y_p(t)]$ / max$[y(t)]$ (Peak Response Positive)
PRN= min $[y_p(t)]$ / min $[y(t)]$ (Peak Response Negative)
PRA = max (PRP,PRN) (Absolute Maximum)

Time History Indicator
Taking $t_0$, $t_1$ = as the times when $I_n = 0.1$ and $I_n = 0.9$ are reached, where $I_n$ is

$$I_n(t) = \frac{\int_0^t (\ddot{x}(\tau))^2 \, d\tau}{\int_0^{t\max} (\ddot{x}(\tau))^2 \, d\tau} \tag{20}$$

we define a metric that measures the quality of the prediction along the time axis as

$$NRMS = \frac{\sqrt{\frac{1}{t_1 - t_0}\int_{t_0}^{t_1} (y(\tau) - y_p(\tau))^2 \, d\tau}}{|y(t)|_{\max}} \qquad (21)$$

## Numerical Illustration of the CS Performance

We illustrate two situations, one where results obtained without filtering are adequate and one where they are not. In both cases we focus on the base shear estimation, which is particularly difficult since it depends on accelerations and these are most affected by higher modes. In the first case we consider a 6 story model with sensors at the base, the roof, and level 3. The fundamental period is 0.65 secs and the excitation is the Parkfield 2004 record (Fault Zone 14). The exact base shear is compared with the CS prediction in Fig.1. As can be seen, the result is accurate.

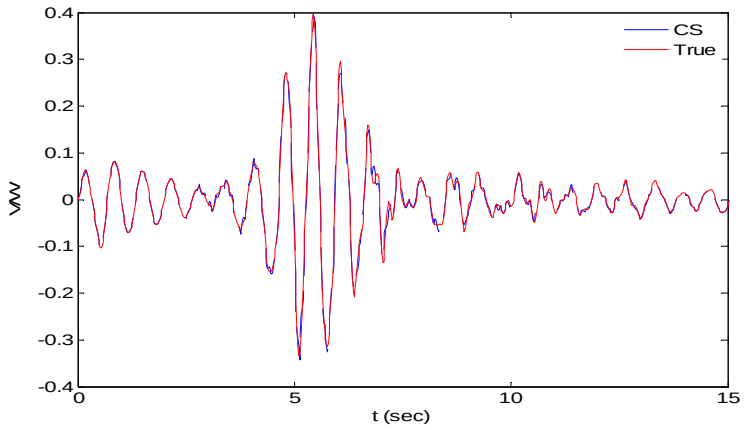


Figure 1. Comparison of the cubic spline estimates base shear and the true values for the 6 story structure under Parkfield 2004

The second example is a 24 story building with sensors at levels 8 and 16 in addition to the base and the roof. The fundamental period is 3 sec and the excitation is the same as before. Fig.2, which compares the exact base shear with the unfiltered CS prediction shows that the results are in this case inaccurate. The high frequency error from the truncated part in Eq.2 is evident.

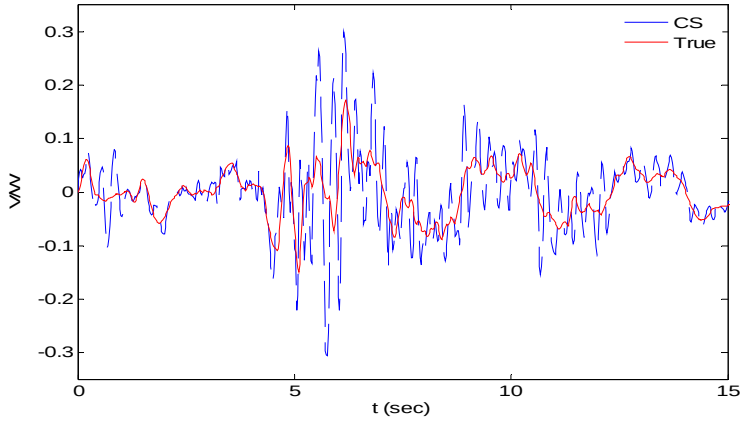


Figure 2.Comparison of the unfiltered cubic spline estimates base shear and the true values for the 24 story structure under Parkfield 2004

Results when a low pass filter with a cutoff frequency at 3 Hz is applied to the measurements are depicted in Fig.3 (the frequency of the 5th mode is 3.07Hz). The post-filter answer is acceptable.

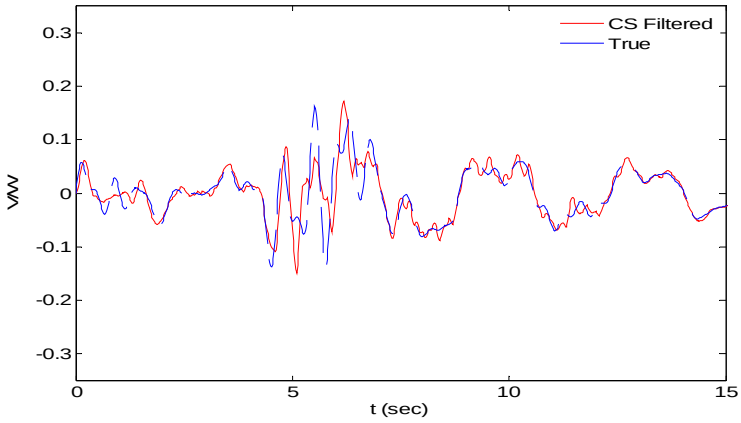


Figure 3. Comparison of the filtered cubic spline estimates base shear and the true values for the 24 story structure under Parkfield 2004

## Model Based Estimation

### The Kalman Filter

The Kalman Filter (Kalman 1960) is the optimal estimator for linear dynamics and measurement processes with Gaussian unmeasured disturbances and measurement noise. The methodology consists of a forecast step and an updating step in which parameters are adjusted to honor the observations. Let the state and output equations for a linear system be given by

$$x_{k+1} = Ax_k + Bu_k + w_k \tag{22}$$

$$y_k = Cx_k + v_k \tag{23}$$

where x is the state, u is a deterministic input, ω are unmeasured disturbances, y is the measured output, *v* is measurement noise and the triplet {A, B, C} are the system matrix, the input to state matrix, and the state to output matrices; ω and *v* are assumed white with covariance matrices $Q_k = E(\omega_k \omega_k^T)$ and $R_k = E(v_k v_k^T)$. The expected value of the state at k=0 is $x_0$ and the covariance of the state error at the origin is $P_0$. The algorithm proceeds as follows:

1. Move forward

$$\hat{x}_{k+1}^- = A\hat{x}_k^+ + Bu_k \tag{24}$$

2. Compute the covariance of the state error prior to incorporating the information from the measurement

$$P_{k+1}^- = AP_k^+ A^t + Q_k \tag{25}$$

3. Compute the Kalman gain

$$K_{k+1} = P_{k+1}^{-} C^t (A P_{k+1}^{-} A^t + R_{k+1})^{-1} \tag{26}$$

4. Update the state using the measurement

$$\hat{x}_{k+1}^{+} = \hat{x}_{k+1}^{-} + K_{k+1}(y_{k+1} - C_{k+1}\hat{x}_{k+1}^{-}) \tag{27}$$

5. Update the covariance of the state error

$$P_{k+1}^{+} = (I - K_{k+1}C)P_{k+1}^{-} \tag{28}$$

6. Repeat from step#1.

The relation between the system mass, damping and stiffness matrices and the state-space matrices {A,B,C} in the previous equations is presented subsequently in Eqs.35-37. As can be seen, in the Kalman filter the discrepancies between the measurements and the model predictions come from the response of the system to the unmeasured input $\omega_k$ (and the measurement noise $v_k$). Note that to apply a Kalman filter the covariance of the process and measurement noise, $Q_k$ and $R_k$ have to be specified. In the seismic reconstruction problem the bulk of the error comes from model approximation and there is no clear basis for selecting $Q_k$ and $R_k$, indicating that the conditions are not those of the standard Kalman filter problem. In the numerical section we use an ad hoc implementation of the Kalman filter based on Q = I and R = 0.

**The RTS Smoother**

The Kalman filter provides an estimate of the state at time t using measurements up to time t. When one is operating offline it is possible to also use measurements after time t. The schemes that use not only past but also future measurements to estimate the state at time t are known as smoothers. Fixed interval smoothers are smoothers that estimate the state at every time station using the same set of data (a fixed time interval). The RTS smoother is a fixed interval smoother introduced by Rauch et al (1965). The algorithm proceeds as follows:

- Perform a standard Kalman filter estimation and store: $x_{k,f}^{-}$ , $x_{k,f}^{+}$ $P_{k,f}^{-}$ and $P_{k,f}^{+}$ , where the subscript *f* is added to indicate that these are results from the *forward* pass of the Kalman filter.

- Compute the smooth estimate of the state, $x_{k,s}$ ,as

$$x_{k,s} = x_{k,f}^{+} + G_k \left( x_{k+1,s} - x_{k+1,f}^{-} \right) \tag{29}$$

where

$$G_k = P^+_{k,f} A^T [P^-_{k+1,f}]^{-1} \tag{30}$$

**The Minimum Norm Response Corrector (MIRC)**

The algorithm presented next is a deterministic scheme that uses pseudo-forces to enforce the measurements. The approach falls in the category of smoothers because the predictions at time t are based on all the measurements (past and future). Let *m* be the number of measurements, *n* be the number degrees of freedom and ℓ the number of time steps. Assuming linear behavior the equations of equilibrium for an accurate representation of the structure can be written as

$$(M + \Delta M)\ddot{q} + (C_{dam} + \Delta C_{dam})\dot{q} + (K + \Delta K)q = b_{2d} P_d(t) + b_{2u} P_u(t) \tag{31}$$

where the matrices in the parenthesis are the true matrices and the triple $\{M,C_{dam},K\}$ are matrices the analyst has selected to represent the system. Implicit in Eq.31 is the fact that we assume the error to be parametric, i.e., that the order of the model is correct. The applied loading is expressed as the sum of two parts: $P_d(t)$, which is known, and a possibly unmeasured component $P_u(t)$, $b_{2d}$ and $b_{2u}$ are the spatial distributions of the known and unmeasured loads and *q* is a vector containing the response at the degrees of freedom. From Eq.31 one has

$$M\ddot{q} + C_{dam}\dot{q} + Kq = b_{2d} P_d(t) + g(t) \tag{32}$$

where the true corrector g(t) is

$$g(t) = b_{2u} P_u(t) - (\Delta M\ddot{q} + \Delta C_{dam}\dot{q} + \Delta Kq) \tag{33}$$

For any estimated corrector $\hat{g}(t)$ one has

$$M\hat{\ddot{q}} + C_{dam}\hat{\dot{q}} + K\hat{q} = b_{2d} P_d(t) + \hat{g}(t) \tag{34}$$

If one neglects measurement error it is evident that the corrector $\hat{g}(t)$ must be such that the response from Eq.34 matches the measurements. From inspection of Eq.33 one does not expect the corrector to be zero at any particular coordinate so in MIRC $\hat{g}(t)$ is taken to be potentially non-zero at all coordinates. Since the number of coordinates is larger than the number of measurements infinite corrector loads can be formulated. In MIRC, as shown next, the corrector sequence is selected such that $[\hat{g}_0 \quad \hat{g}_1 \quad . \quad \hat{g}_\ell]$ has minimum norm (smallest singular value).

**MIRC Algorithm**

Here we show only the computational steps on the basis that the measurements are relative velocities, for a more detailed description of the derivation see (Bernal and Nasseri 2009).

1) Form the matrices

$$A = \begin{bmatrix} 0 & I \\ -M^{-1}K & -M^{-1}C_{dam} \end{bmatrix} \tag{35}$$

$$B = \begin{bmatrix} 0 \\ M^{-1}b_{2f} \end{bmatrix} \tag{36}$$

$$C = \begin{bmatrix} 0 & C_v \end{bmatrix} \tag{37}$$

where $C \in R^{mx2n}$ and $C_v \in R^{mxn}$ is a matrix of zeros with a 1 in each row at the column position corresponding to the measured coordinate. For example, in a 10 story building with sensors in levels 3 6 and 10

$$C_v = \begin{bmatrix} 0 & 0 & 1 & 0 & 0 & 0 & 0 & 0 & 0 & 0 \\ 0 & 0 & 0 & 0 & 0 & 1 & 0 & 0 & 0 & 0 \\ 0 & 0 & 0 & 0 & 0 & 0 & 0 & 0 & 0 & 1 \end{bmatrix}$$

$b_{2f}$ gives the spatial distribution of the corrective forces, which, the typical MIRC applications is taken as the identity.

2) Compute

$$A_d = e^{A\Delta t} \tag{38}$$

$$B_d = (A_d - I)^2 A^{-2} B \frac{1}{\Delta t} \tag{39}$$

$$D_d = -CA^{-1}\left[ I - A^{-1}(A_d - I)\frac{1}{\Delta t} \right] B \tag{40}$$

$$Y_j = CA_d^{j-1}B_d \qquad j = 1,2,...,k \tag{41a}$$

$$Y_0 = D_d \tag{41b}$$

and form

$$H_l = \begin{bmatrix} Y_0 & 0 & \dots & 0 \\ Y_1 & Y_0 & \dots & 0 \\ & & \dots & \\ Y_l & Y_{l-1} & \dots & Y_0 \end{bmatrix} \tag{42}$$

with $\Delta t$ = time step.

3) Compute the difference between the measurements and the predictions of the model $z_2$ (in this presentation assumed to be relative velocities) and place them as columns of the matrix Z, namely

$$Z_l = vec\left[z_2(0)\ \ z_2(1)\ \ z_2(2)...z_2(l)\right] \tag{43}$$

where *vec* is an operator that stacks the column of a matrix in a single one.

4) Calculate the corrective loads as

$$F = H_l^{-*}.Z_l \tag{44}$$

where

$$F = vec\left[\hat{g}_1\ \ \hat{g}_2\ \ \hat{g}_3\ \ ...\ \ \hat{g}_l\right] \tag{45}$$

Numerical Illustration

Consider the 24 story structure use in the plots of Figs 2 and 3. To reflect error in the model we formulate a nominal model based on a shear-flexural idealization (Miranda and Taghavi 2005) and treat the frame structure as the "truth model". We adjust the properties of the nominal model so the period of the first mode is correct. The left side of Fig.4 compares the base shear predicted by the model with the true values and the right side illustrates the comparison with the MIRC estimate. In this case the error in the nominal model is not large but the improvement realized by MIRC is evident.

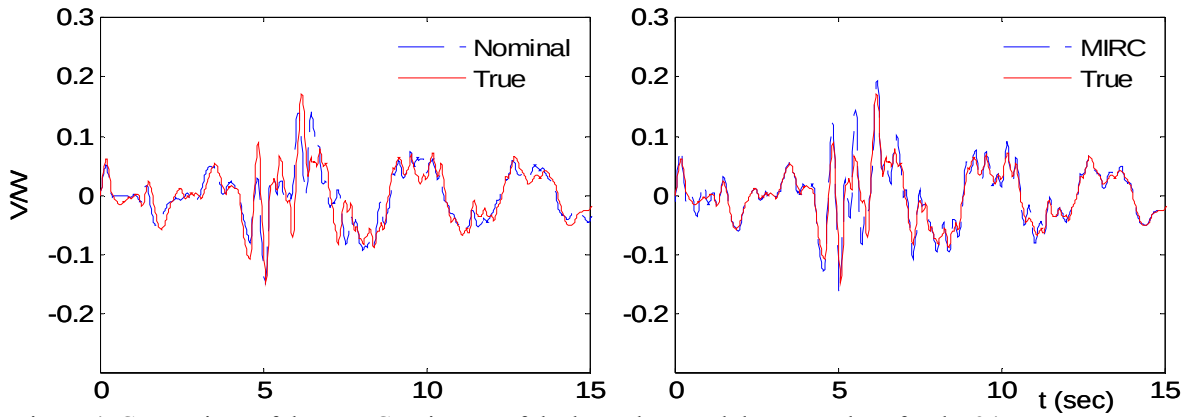


Figure 4. Comparison of the MIRC estimates of the base shear and the true values for the 24 story structure under Parkfield 2004 earthquake

Observation

A consistent approach to compute the story shears when MIRC is used is to take them as the sum of the forces (from the top down) compatible with the displacement response. This procedure is equivalent to computing the shears as the sum of the inertial forces plus the contribution of the fictive corrective forces. Numerical experience has shown, however, that the story shears computed exclusively using the accelerations are generally more accurate and this is how they are computed in the numerical section.

## Nonlinear Response

The effect of nonlinearity on the quality of the response reconstruction depends on the estimation method and on whether the nonlinearity produces drastic changes in the dominant shape of the response (i.e., if it is highly concentrated) or not.

### Basis Fitting

One expects accuracy to diminish more notably if the nonlinearity is strongly localized. To illustrate, suppose that there is a 2-story structure whose roof and base are instrumented. The CS estimate of the 1st floor is in this case the average of the two measurements. If nonlinearity is restricted to the 1st floor the response will be under-predicted but if it takes place only on the second it will be over predicted. Fig.5 depicts results for the drift in the first level of the 6-story structure used previously for two distributions of the nonlinearity: a) nonlinearity restricted to the 1st level and b) nonlinearity spread throughout the frame. As can be seen, the CS interpolator provides a much better estimation when the nonlinearity is distributed.

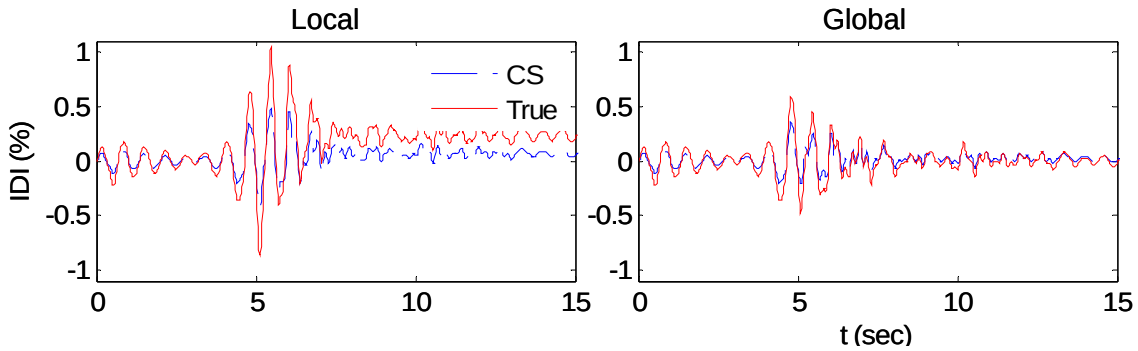


Figure 5. Effects of local and global nonlinearity on the estimation of the 1st story IDI of the 6 story structure.

### The MIRC

It is interesting to note that while the MIRC is based on the superposition principle, the response correction based on a linear model can still provide improve estimates of nonlinear response. To illustrate, Fig. 6 shows the MIRC estimates of the 1st floor IDI based on a linear model when the true system response is nonlinear. As can be seen, the MIRC results try to follow the residual displacement.

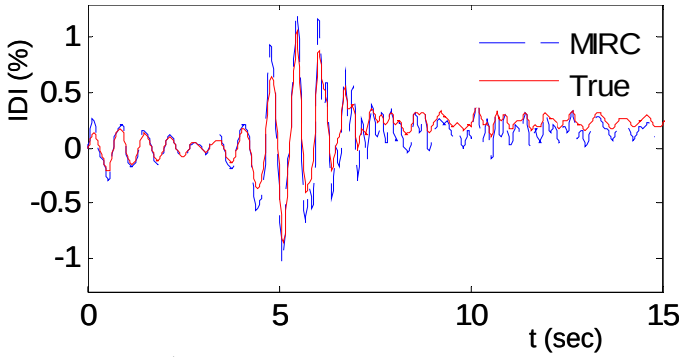


Figure 6: Comparison of the estimates of1st floor IDI of the 6story nonlinear model using a linear MIRC

## Numerical Results

Three dimensional nonlinear models of 3 instrumented buildings were used as surrogates of the real structures. The buildings are the 13 story Sherman Oaks (CSMIP # 24322), the 10 story San Jose building (CSMIP # 57356) and the 6 story Burbank building (CSMIP # 24370). The instrumented levels and other details can be found at (http://www.strongmotioncenter.org/). The responses of the nonlinear models to an ensemble of 30 ground motions were treated as the true responses. In the case of model based estimation the nominal model was taken as a linear shear building with properties adjusted to match the first mode period. Since the variation of the error indicators with height is not too significant the data for all floors (for shear and IDI) were treated together. After excluding the shears at the last level (since it is determined by the measured roof acceleration, and the IDI of floors for which there are adjacent sensors) the data set consisted of 1560 histories of story shears and 1260 histories of IDI. The data set was not separated into linear and nonlinear responses because in practice estimators are used without this information. The limits of the range for which the central 80% of the probability distribution function, as defined in Fig.7, are reported in Figs.8 and 9.

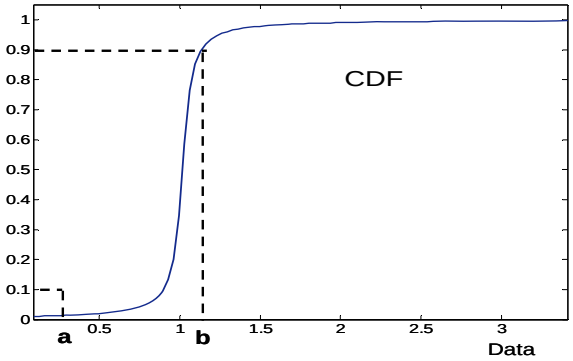


Figure 7: Definition of the parameters *a* and *b* that define the central 80% of the probability distribution functions

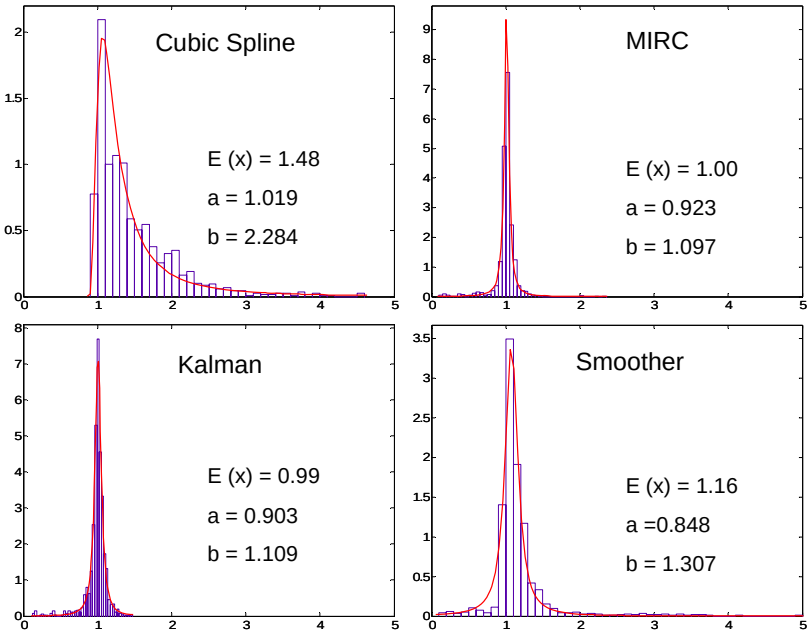


Figure 8: Probability distributions for the PRA of the story shears for various estimators

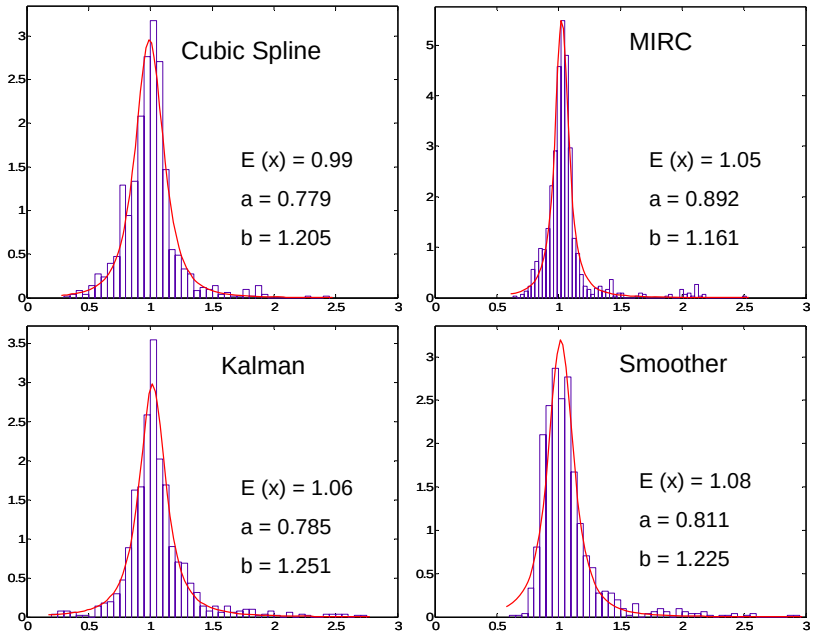


Figure 9: Probability distribution for the PRA of IDI for various estimators

The results shown suggest that the MIRC provides the best estimates. Fig 10 shows the mean and the standard deviation for the NRMS.

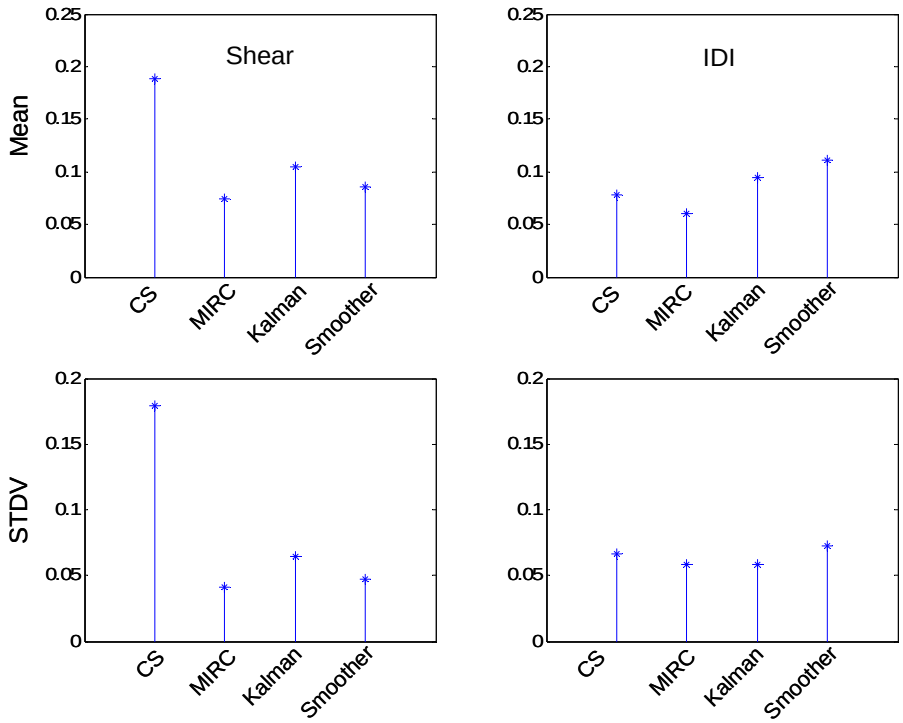


Figure 10: Mean and the STDV of the NRMS of shear and IDI for various estimators

## Conclusions

It is shown that the cubic spline reconstruction is a particular case of the basis fitting approach wherein the basis is implicitly selected by the positioning of the sensors. This result clarifies the conditions when the scheme can be expected to give accurate predictions and when it cannot. It is contended, specifically, that the cubic spline interpolation is adequate when the number of modes that contribute to the quantity of interest is less than the number of sensors (not including the base). The result on the basis fitting analogy is computationally significant because it shows that the interpolating coefficients of the spline need not be computed at each time step, as has been done in the traditional implementation. Although not necessary when the contribution of higher modes is negligible, it is shown that low pass filtering of the measurements, prior to obtaining the cubic spline reconstruction, is good practice. Nonlinearity typically reduces the accuracy attained because the truncated basis needed to fit the nonlinear response can differ substantially from the linear one (which is best approximated by the spline basis). Reductions in accuracy are particularly important when the nonlinearity is concentrated in a few levels. When the number of sensors is not sufficient much improved accuracy over the cubic spline can be realized by using estimators that blend the measurements with a nominal model. Of the estimators examined in this study the one that proved most effective reconstructs the response using the nominal model, the ground excitation and a set of fictive forces of minimum norm that enforce the measurements.

The numerical results show that the cubic spline is generally adequate for estimating inter-story drift but tends to over-predict story shears. These observations are anticipated by the theory and derive from the fact that for typical sensor layouts, and typical structures, the number of modes with a significant contribution to drift is smaller than for the accelerations needed to compute story shears. It appears, based on the 1560 histories obtained, that the overestimation of story shears by the spline can be quite significant. Specifically, values in excess of 2 for the ratio of the estimation to the true value were computed in more than 10% of the cases. For the MIRC estimator, in contrast, the threshold separating the largest 10% ratios was only 1.1.

## References

Alimoradi, A., Miranda, E., Taghavi, S. And Naeim, F. (2006). “Evolutionary model identification utilizing coupled shear-flexural response-Implications for multistory buildings. Part 1:Theroy”, *J. Structural Design of Tall Spec. Buildings*, 15, p.51-65.

Bernal D., Nasseri, A. (2009). “An approach for response reconstruction in seismic applications”, *Proceedings of the 3rd International Operational Modal Analysis Conference IOMAC09,* Ancona Italy May 4-6 2009.

De la Llera, J.C., Chopra, A.K. (1995). “Evaluation of seismic code provisions using strong-motion building records from the 1994 Northridge earthquake.”, *SMIP95 Seminar on Seismological and Engineering Implications of Recent Strong-Motion Data*, pp. 25-40.

Hernandez E., and Bernal D. (2008) "State estimation in systems with modal uncertainties", *Journal of Engineering Mechanics*, ASCE , v.134,n.3,pp.1-6. (in press).

Kalman, R.E. (1960), "A new approach to linear filtering and prediction problems", *ASME Journal of Basic Engineering* ,v.82 , n.1, pp. 35-45.

Li, Y. and Mau, S.T., (1997). "Learning from recorded earthquake motion of buildings.", *J. Structural Eng.*, ASCE, v. 123 n. 1, pp. 62-69.

Limongelli, M.P. (2003). "Optimal location of sensors for reconstruction of seismic responses through spline function interpolation", *Earthquake Engineering and Structural Dynamics*, v. 32, pp. 1055-1074.

Lui, R.R., Mahin, S. , Moehle,J. (1990). "Seismic Response and Analytical Modeling of the CSULA Administration Building Subjected to the Whitter Narros Earthquake.", *SMIP 1990 Seminar on Seismological and Engineering Implications of Recent Strong-Motion Data*, pp. 8-1 - 8-10.

Miranda, E. and Taghavi, S., (2005). "Approximate floor acceleration demands in multistory buildings. I:formulations", *J. Structural Eng*., ASCE, v. 131 n. 2, pp. 203-211.

Naeim, F. (1997), Performance of instrumented buildings during the January 17, 1994 Northridge earthquake—an interactive information system, *Report No. 97-7530.68, John A. Martin and Associates, Inc.*.

Naeim, F., Lee, H., Hagie, S., Bhatia, A., Alimoradi, A., and Miranda, E., (2006), "Three dimensional, real time visualization and automated post-earthquake damage assessment of buildings", *Structural Design Tall and Special Buildings*, v.15 , pp. 105-138.

Rauch, H., Tung, F. and Striebel, C., (1965). "Maximum likelihood estimates of linear dynamic systems", *AIAA Journal* v.3, n.8. pp. 1445-1450

Ventura, .C.E. and Ding, Y. 2000. "Linear and nonlinear seismic response of a 52-story steel frame building.", *J. Structural Design of Tall Buildings*, v. 9, n.1, pp. 25-45.

Ventura, C.E. , Laveric, B., Brincker, R. and Andersen, P., 2000. "Comparison of dynamic characteristics of two instrumented tall building." *Proc. 21st Int. Modal Analysis Conference* (IMAC).